THE JOURNAL OF PHYSICAL CHEMISTRY B

Article

pubs.acs.org/JPCB

More Evidence on the Control of Reverse Micelles Sizes. Combination of Different Techniques as a Powerful Tool to Monitor AOT Reversed Micelles Properties

Andrés M. Durantini, R. Darío Falcone, Juana J. Silber, and N. Mariano Correa*

Departamento de Química, Universidad Nacional de Río Cuarto, Agencia Postal # 3. C.P. X5804BYA Río Cuarto, Argentina

Supporting Information

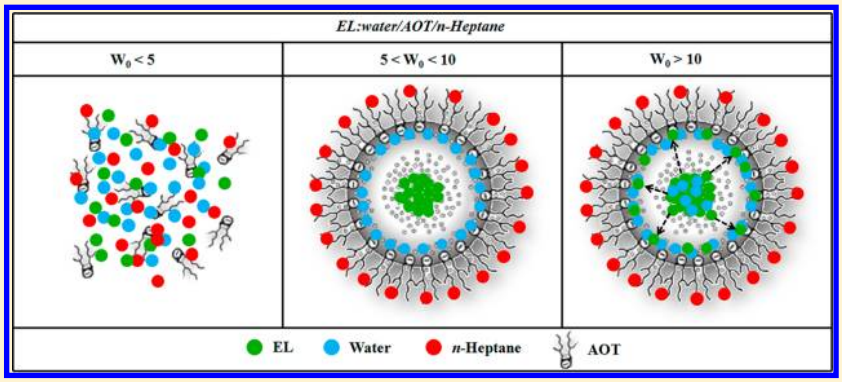

ABSTRACT: In this work, we have investigated the behavior of 4-aminophthalimide (4-AP) in solvent mixtures of ethyl lactate (EL)− water and EL−*n*-heptane and in reversed micelles (RMs) media made of EL−water/sodium 1,4-bis(2-ethylhexyl)-sulfosuccinate (AOT)/*n*-heptane. We have used dynamics light scattering (DLS) and absorption, steady-state and time-resolved emission (TRES) techniques. 4-AP is a very interesting and unique molecule used to study preferential solvation in water mixtures since its emission profile changes dramatically when its sphere shell is solvated by water molecules. Thus, in homogeneous media 4-AP is strongly solvated by water in the EL−water mixture and by EL in the EL−*n*-heptane mixture, results that show the importance of the hydrogen bonding in the 4-AP solvation. We were motivated by this feature of 4-AP and have used it to monitor properties in AOT RMs. Thus, we use 4-AP spectroscopic behavior in conjunction with DLS technique to reveal the location of each polar solvent of the mixture encapsulated within the RMs media. We found that in the EL−water/AOT/*n*-heptane RMs the results strongly depend on the amount of water dissolved. Below W_0 = [water]/[AOT] = 5, there are no reversed micelles and EL, water, AOT and *n*-heptane forms a nonstructured mixture. For W_0 values between 5 and 10, the droplet sizes are independent of the EL content because of its strong intermolecular interactions forms an EL polar core and only water is found at the interface. For W_0 values higher than 10, the droplets size increase with the EL content and EL molecules are detected at the AOT RMs interface. We inferred that the RMs sizes will change only if the polar solvent encapsulated interacts with the interface changing the surfactant packing parameter. Then, we can assume that it is possible to create RMs with solvents that do not interact with the interface but can be encapsulated in the polar core. These results, give evidence that expand the knowledge about which are the factors that determine when RMs droplet sizes changes with the polar solvent content, giving insights that will help to control the sizes of the AOT RMs. This will open diverse avenues since RMs are interesting nanoreactors for heterogeneous chemistry, templates for nanoparticles and models for electron transfer reaction that happens in membranes.

INTRODUCTION

Reverse micelles (RMs) are aggregates of surfactants formed in nonpolar solvents. The polar head groups of the surfactants point inward and the hydrocarbon chains point toward to the nonpolar medium.[1−3] A common surfactant used to form RMs is sodium 1,4-bis(2-ethylhexyl)sulfosuccinate (AOT, Scheme 1). The RMs formed with this surfactant can solubilize a large quantity of water in a wide range of nonpolar solvents, reaching values of W_0 = [water]/[AOT] as large as 40−60 depending on the nonpolar solvent, the solute and the temperature.[1−3] RMs can be interesting nanoreactors for heterogeneous chemistry, as well as templates for nanoparticles and models for biological membranes.[4] Besides water, some polar organic solvents, having high dielectric constants and very low solubility in hydrocarbon solvents, can also be encapsulated in RMs. The AOT/*n*-heptane RMs containing these solvents are known to be spherical and, it has been demonstrated that the size of the RMs depends on the W = [polar solvents]/[AOT] values.[5]

Received: December 3, 2012
Revised: March 2, 2013
Published: March 11, 2013

Scheme 1. Molecular Structure of AOT, EL, and 4-AP

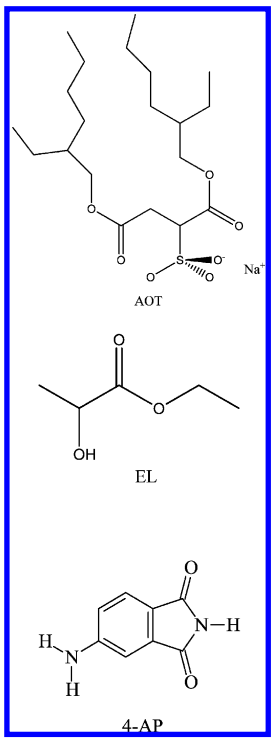

The study of hydrogen bond molecular interactions of binary mixtures containing glass forming liquid solvents is currently a significant challenge in the research of soft condensed matter science because of their wide applications in the field of science and technology.[6] As a result of the intermolecular interactions, preferential solvation of solutes in mixed solvents may be observed. This term applies if the local mole fractions of the solvent components in a solvation microsphere surrounding the solute differ from the bulk ones.[7−10] In this direction, we have been interested in the study of the effect that AOT RMs has on the solvent−solvent and solvent−surfactant interaction of polar solvent mixtures upon encapsulation.[10] We have demonstrated how the confined environment affects dramatically the interaction between two different polar solvents: glycerol (GY) and dimethylformamide (DMF); in homogeneous media, GY and DMF interact strongly through hydrogen bond interactions while the opposite is found when the mixture is encapsulated inside AOT RMs. Upon confinement of the GY−DMF mixture and because the strong GY−AOT interaction, GY strongly binds through hydrogen bond to the AOT SO_3^- group at the interface and DMF makes complexes with the Na^+ counterions in the polar core of the aggregates diminishing significantly the bulk GY−DMF interaction. Therefore, each solvent (in the mixture) behaves as non-interacting solvents inside RM.[10]

Searching for new solvents to create RMs, ethyl lactate (EL, Scheme 1) emerges as an alternative green solvent since it is 100% biodegradable, it does not show any potential health risk, it is easy recyclable, noncorrosive, and, in case of vapors release is non-ozone-depleting. EL has the ability to develop intramolecular hydrogen bonding among neighboring hydroxyl and carbonyl groups, and this interaction competes with the intermolecular hydrogen bonding with other EL molecules and/or with water in mixtures.[11−13] It may be obtained from carbohydrate feedstocks at very low and competitive prices. Moreover, the use of carbohydrates as a starting point in its production leads to a renewable product, and thus sustainable, not rising from petrochemical sources.[14] Furthermore, EL is produced at industrial level from the esterification of lactic acid with ethanol using different procedures leading to EL and water mixtures, products from which pure EL may be obtained.[11,13] Thus, the knowledge of the properties of the EL−water mixtures is crucial for the industry.

One way to assess to study liquid−liquid interactions for solvent mixtures under confinement such as in AOT RMs is the use of molecular probes. We have chosen an interesting probe, 4-aminophthalimide (4-AP, Scheme 1), which has an electron donor (amino group) and an electron acceptor moiety (carbonyl group) placed in conjugated position in the benzene ring which upon electronic excitation significantly change the electron density distribution.[9,15−17] 4-AP has been extensively used as strong fluorescent probe in different environments including nanomaterials, organized media and biological systems.[17−26] It is known that 4-AP is an excellent probe because its fluorescence lifetimes, spectra and quantum yields are affected greatly by the environment properties.[16,26] Very recently, we have demonstrated that the 4-AP behavior is unique in water.[27] The strong dependence of the emission band with the excitation wavelength found in water did not receive adequate attention in earlier works. Thus, we want to take advantages on this unique feature in order to investigate complex systems like RMs.

With this background and in the context of our studies in RMs, we consider worthy to investigate the effect that the confinement has on the interaction between EL and water. The study was performed in homogeneous and in AOT/*n*-heptane RMs media. To achieve this goal we have used the solvatochromic behavior of the molecular probe 4-AP. It must be noted that 4-AP was used before to investigate the water structure in water/AOT/*n*-heptane RMs but only one absorption band was monitored.[18] We performed absorption, steady-state and time-resolved fluorescence (TRES)[15] using different excitation and emission wavelengths. We also use dynamic light scattering (DLS) to demonstrate that the AOT RMs are effectively formed. The results will show where are located the sequestrated EL and water molecules within the RMs.

MATERIALS AND METHODS

Materials. Ultrapure water was obtained from Milli-Q filtered, 18.2 MΩ cm resistivity. Ethyl lactate (EL) and *n*-heptane of the highest grade available (Aldrich spectral of HPLC grade) were used as received. The molecular probe 4-aminophthalimide (4-AP, Aldrich) was purified by repeated recrystallization from ethanol.[16]

Sodium 1,4-bis(2-ethylhexyl)sulfosuccinate (AOT) from Sigma (>99% purity) was dried under reduced pressure, over P_2O_5 until constant weight prior use. The UV−vis spectra of 1-methyl-8-oxyquinolinium betaine in the presence of AOT RMs showed that the surfactant is free of acidic impurities, which would have greatly reduced the intensity of the band at 502 nm.[28,29]

Methods. The EL−water and EL−*n*-heptane solutions at any solvent bulk mole fraction values composition, X_{water} or $X_{n\text{-hp}}$, studied were prepared by weight.

The stock solutions of AOT in *n*-heptane were prepared by weight and volumetric dilution. To obtain optically clear solutions they were shaken in a sonicating bath and, the polar solvents were added using a calibrated microsyringe. The surfactant solution was 0.10 M in *n*-heptane. For any X_{water} value studied, the amount of polar solvents present in the system is expressed as the molar ratio between EL and the AOT concentration W_{EL} = [EL]/[AOT] while the amount of

dx.doi.org/10.1021/jp311882t | J. Phys. Chem. B 2013, 117, 3818−3828

Scheme 2. Emission Mechanism and the Solvent-Mediated Proton Transfer for 4-AP in Water at Any Excitation Wavelength. $S_0'_{enol}$ Represents the Unstable with a Short Lifetime enol-ICT Ground State Species that Rapidly Converts to S_0 (Ref 27)

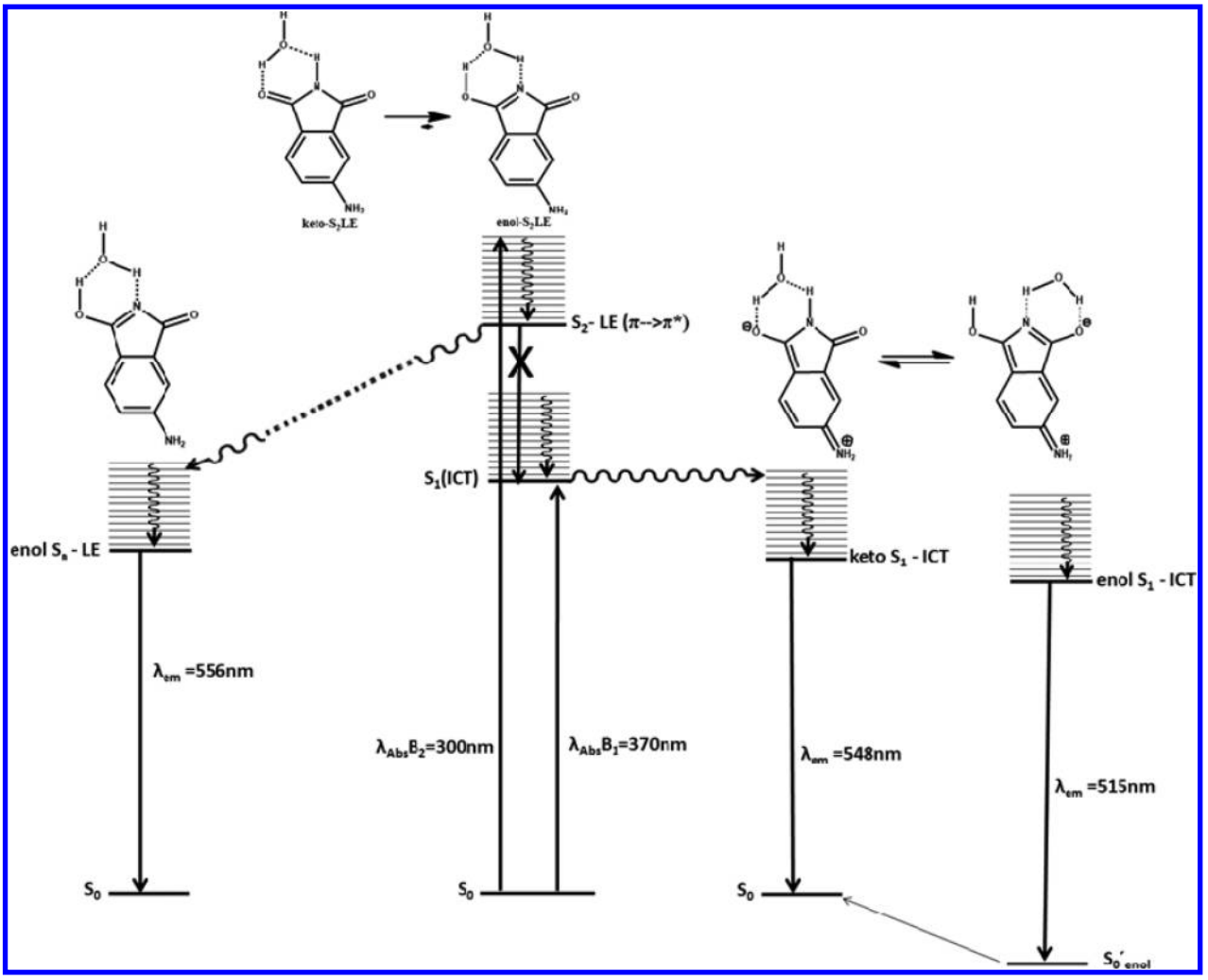

water is expressed as the molar ratio between water and the AOT concentration W_0 = [water]/[AOT].

To introduce the probe, a 0.01 M solution of 4-AP was prepared in methanol (Sintorgan HPLC quality). The appropriate amount of this solution to obtain a given concentration of the probe in the homogeneous or micelle medium was transferred into a volumetric flask, and the methanol was evaporated by bubbling dry N_2; then, the suitable EL–water mixtures or the AOT RMs solution was added to the residue.

General Data. The absorption spectra were measured by using Shimadzu 2401 equipment at 25 °C unless otherwise indicated. A Spex fluoromax apparatus was employed for the fluorescent measurements. Corrected fluorescence spectra were obtained using the correction file provided by the manufacturer. The path length used in the absorption and emission experiments was 1 cm. Because the absorption and emission bands are broad the λ_{max} was measured by taking the midpoint between the two positions of the spectrum where the absorbance is equal to 0.9 x A_{max}. Thus, the uncertainties in λ_{max} are about 0.1 nm.

Fluorescence decay data were measured with the time correlated single photon counting technique (TCSPC) (Edinburgh Instrument FL-900) with a PicoQuant subnanosecond Pulsed LED PLS 370 (emitting at 378 nm) < 600 ps fwhm. Fluctuations in the pulse and intensity were corrected by making an alternate collection of scattering and sample emission. The quality of the fits was determined by the reduced χ^2 and for the best fit χ^2, must be around 1.0.[30] It must be noted that in any exponential fit (mono or bi), we have tried to perform multi- or monoexponential fitting but the statistic of the decays were not improved or, became worse.

Time-resolved emission spectra, TRES, were generated from a set of emission decay times taken at 10 nm intervals spanning the fluorescent spectrum (typically 20 decays). To resolve the convolution with the instrument response on the time-resolved decay data at each emission wavelength, a multiexponential fit was used. The purpose of these fits is simply to represent the decay curves and no physical meaning is ascribed to the derived exponential parameters.[15] Two components were generally required to obtain a satisfactory fit to the data. TRES have been constructed following the procedure described in the literature.[15,31]

The apparent hydrodynamic diameters (d_{App}) of the different AOT RMs were determined by dynamic light scattering (DLS, Malvern 4700 with goniometer and 7132 correlator) with an argon-ion laser operating at 488 nm. Multiple samples at each size were made, and 30 independent size measurements were made for each individual sample at the scattering angle of 90°. The algorithm used was CONTIN, the d_{App} values reported were weighted by intensity, volume and/or number since no differences are observed. The DLS experiments show that the polidispersity of the AOT RMs size is less than 5%. All the experiments were carried out at 25 ± 0.5 °C.

RESULTS AND DISCUSSIONS

1. Absorption and Emission Studies in Homogeneous Solvent Mixtures: 4-AP in EL–Water and EL–*n*-Heptane mixtures. It has been reported that the bathochromic shift of

dx.doi.org/10.1021/jp311882t | J. Phys. Chem. B 2013, 117, 3818–3828

the emission spectra of 4-AP in protic solvents is much greater than the one observed in aprotic ones and, the greatest bathochromic shift being detected in water. It is believed that during 4-AP excitation there is a redistribution of the charge yielding to an internal charge transfer state (S_1−ICT). As a consequence there is a significant change in the energy of the hydrogen bonds with the protic solvents that are already present in the ground state.[16,17] Thus, the Stokes shift of this S_1−ICT emission is very sensitive to the polarity and hydrogen bond donating ability of the medium. Also, the S_1−ICT character of the transition causes the dipole moment increase upon excitation from 3.5 to 6.5 D.[16,32] Also, it was demonstrated that the absorption and emission bands shifts bathochromically as the polarity/polarizability and the hydrogen bond abilities of the solvents increases. Moreover, the susceptibility to the specific interactions increases upon 4-AP excitation.[16,23,27] Very recently we have demonstrated that the 4-AP behavior is unique in water.[27] The 4-AP absorption spectra consist in two bands that correspond to different electronic transitions: the band around 300 nm is the $S_0 \rightarrow S_2$ ($\pi-\pi^*$: S_2-LE) transition (B2 band) and, the band around 370 nm is the $S_0 \rightarrow S_1$ (S_1−ICT) transition (B1 band). Moreover, in all the organic solvents studied, the emission spectra (steady and time-resolved) are the same independently of the excitation wavelength used, i.e., B1 or B2, which is the expected behavior for a fluorophore emitting from its lowest excited state (S_1−ICT). However, in water the emission spectra peaks different depending on the excitation wavelength used. While the fluorescence decays of 4-AP in water exhibit no emission wavelength dependence at λ_{excB2} the situation is quite different when λ_{excB1} is used. Also, we found a time-dependent emission spectrum that shift to the blue with time. We explain the 4-AP photophysics in all the solvents studied considering the solvent proton transfer reaction upon excitation to the 4-AP excited state. When λ_{excB2} is used and the S_2-LE is populated, water is the only solvent that produces the enol S_2 LE species that cannot yield the S_1−ICT state and the emission comes from the relaxed enol excited state (See Scheme 2). On the other hand, when λ_{excB1} is used the S_1−ICT state is populated and the emission arises from the keto and enol S_1−ICT states. The latter species goes to a very well stabilized ground state with the consequent increase in the electronic transition energy gap.[27]

With regard to solvent mixtures, 4-AP was used before to investigate preferential solvation in water−dioxane,[23] toluene−acetonitrile,[16] and toluene−ethanol[16] systems. In the non aqueous mixtures it was demonstrated strong preferential solvation of 4-AP by ethanol[16] but, in the water−dioxane mixture the authors claimed no preferential solvation of the probe by water molecules. The solvathochromic behavior found in the mixture was shown to be controlled by hydrogen bond abilities of the solvent.[23] Nevertheless, in that investigation,[23] only one absorption band was monitored, and knowing that 4-AP emission profile in water depends strongly on the excitation wavelength used,[27] we believe that to study aqueous solvent mixtures is necessary to use also the B1 absorption maxima as excitation wavelength.

EL has the ability to develop intra- and intermolecular interaction through hydrogen bonding,[13] and it is completely soluble in water and in *n*-heptane, the nonpolar solvent used to create the AOT RMs media. Thus, we study the solvathochromism of 4-AP not only for the EL−water but also for the EL−*n*-heptane solvent mixtures. The idea is to understand hydrogen bond interaction in these mixtures before the more complex RMs systems will be formed.

The 4-AP absorption and emission spectra (at λ_{exc} = B1 maximum band) in pure water and pure EL are shown in Figure S1, parts A and B, respectively, in the Supporting Information. As can be observed, 4-AP presents two absorption bands that correspond to different transitions as was explained, and the emission spectra consist of a single band. The absorbance maxima of B2 and B1 bands in pure water are $\lambda^{max}_{abs\ B2}$ = 303.7 nm and $\lambda^{max}_{abs\ B1}$ = 370.0 nm while at $\lambda_{exc\ B2}$, λ^{max}_{emi} = 561.7 nm, and at $\lambda_{exc\ B1}$, λ^{max}_{emi} = 545.7 nm.[27] In pure EL, the absorbance maxima of B1 and B2 bands are $\lambda^{max}_{abs\ B2}$ = 309.1 nm and $\lambda^{max}_{abs\ B1}$ = 365.4 nm, while the maxima of the emission band at λ_{exc} B2 and λ_{exc} B1 are the same and λ^{max}_{emi} = 526.5 nm.

Parts A and B of Figure S2 in the Supporting Information show the plot of the 4-AP maxima absorbance frequencies for the EL−water and EL−*n*-heptane binary mixtures as a function of the water bulk mole fraction, X_{water}, and *n*-heptane bulk mole fraction, $X_{n\text{-hp}}$ respectively. In this case and because of 4-AP is not soluble in pure *n*-heptane, the $X_{n\text{-hp}}$ values were varied from 0 to 0.75. Parts C and D of Figure S2 in the Supporting Information show the plot of the 4-AP maxima emission frequencies as a function of X_{water} and $X_{n\text{-hp}}$ respectively.

In the aqueous mixtures (Figure S2A, Supporting Information), it can be seen that the absorption B1 band is more sensitive to the water addition than the B2 band. This is the expected since the Kamlet−Taft analysis[33] performed on these bands show greater sensitivity of the maxima of B1 band to the polarity/polarizability and hydrogen bond interactions in comparison with the maxima of B2 band.[27] Also, it is notorious that, in the absorption and emission frequencies plots (Figure S2, parts A and C, Supporting Information), the experimental points deviate from linearity in the whole X_{water} range studied. Moreover, the data are similar to those obtained in pure EL in the EL rich region while, the strongest deviation happens in the water rich region. The results are in agreement to those proposed by Aparicio et al[13] where the addition of small quantities of EL to water has a strong effect on the water structure reinforcing the water networks whereas for the EL-rich region the addition of water has less remarkable effects.[13] It is interesting to see that the 4-AP solvation by the EL−water mixture in its ground state seems to have a synergist[8,9] effect because the experimental points lie below the pure solvent values at any composition (Figure S2A, Supporting Information). Data from the 4-AP emission profile are in concordance to what was found in the 4-AP absorption spectra discussed. Figure S2C, Supporting Information, shows that 4-AP ICT excited state sense water molecules only in the water rich region.

With regard to the EL−*n*-heptane mixtures, parts B and D of Figure S2, Supporting Information, show that independently on the *n*-heptane content 4-AP is mostly solvated for EL solvent because the strong hydrogen bond interaction between the probe and EL.

Thus, it is clear that 4-AP is almost exclusively solvated by EL molecules in the EL−*n*-heptane mixtures but which is the solvent composition on the 4-AP solvent shell in the EL−water mixture? Figure S3 in the Supporting Information shows the dependence of the 4-AP maximum emission wavelength with the excitation wavelength for different EL−water mixtures. Also the values for EL−*n*-heptane mixtures as well as for pure water and pure EL were included for comparison. As can be seen, in

dx.doi.org/10.1021/jp311882t | J. Phys. Chem. B 2013, 117, 3818−3828

the EL–water mixtures, there is a blue shift of the emission band as the excitation wavelength has lower energy. This is what was found in pure water, where the blue shift of the emission band is around 35 nm.[27] Thus, in the EL–water mixtures, the blue shift of the emission band is less than in pure water and it decreases with the EL content, being almost negligible for mixtures with water content less than 20%. Interestingly, the data never match the values obtained in pure EL. We have explained this distinct behavior in water considering that there are two different emitting species for the 4-AP ICT excited states, with water being the only solvent that can undergo the proton transfer reaction for the ICT excited state, yielding the enol-ICT and the keto-ICT species.[27] Thus, the more stable excited state is the enol-ICT that emits to a ground state (S_0') that is different and more stabilized by water molecules than the one formed by the keto-ICT species emission (Scheme 2).[27] The fact that the effect is detected in any EL–water mixture investigated for water contents higher than the 20% means that water is the solvent that preferential solvates 4-AP. However, at lower water contents EL is the solvent that solvates the molecular probe.

On the other hand, the blue shift is not observed in neat EL and in its *n*-heptane mixtures. In EL–*n*-heptane mixtures the emission maxima values matches the emission maxima found in neat EL at any solvent mixture composition. EL although is a hydrogen bond donor solvent is not able to produce the proton transfer to yield the 4-AP enol-ICT species (Scheme 2) and the emission is from the keto-ICT state as in any other protic or aprotic media.[27]

In order to gain more information on the 4-AP photophysics in the mixtures we study also its behavior in the same systems using time-resolved emission measurements (TRES). TRES is frequently used to study the excited state dynamics and kinetics of fluorescent molecules in solution.[15] The time dependent decays at different emission wavelengths were used to construct the TRES spectra and, the results are shown in Figure S4, parts A, B, and C, in the Supporting Information section. Figure S4A (Supporting Information) shows typical results for the TRES spectra in the 1:1 EL–water mixture at λ_{exc}= B1 maximum band. The TRES spectra for pure EL and for the 1:1 EL–*n*-heptane mixtures are shown in Figure S4, parts B and C, Supporting Information, respectively. As can be seen, in the EL–water mixture, the 4-AP behavior is similar to the one found in pure water,[27] and with an increase in the time, the band shape narrows and the emission spectra shift progressively to shorter wavelengths (blue shift) due to the presence of the two 4-AP ICT emitting species (Scheme 2).[27] On the other hand, in pure EL and in the EL–*n*-heptane mixtures there is no dependence with time indicating that the solvation dynamics is too fast to be detected in our nanosecond setup and, that 4-AP emits only from the relaxed keto-ICT state.

2. EL–Water/AOT/*n*-Heptane Reversed Micelles. *2.1. DLS Studies.* In our work, all the DLS experiments were carried out at a fixed AOT concentration of 0.1 M and the RMs solutions are not at infinite dilution. Nevertheless we think appropriate to introduce an apparent hydrodynamic diameter (d_{App}) in order to make the comparison of our systems. A similar approach was used previously.[34,35] Also, in order to clarify the presentation of our data in the AOT RMs, we will use the following nomenclature: the amount of water will be denoted as W_0 = [water]/[AOT] and the amount of EL will be denoted as W_{EL} = [EL]/[AOT]. Thus, in our experiments we have fixed the values of W_0 or W_{EL} if the amount of water or EL is investigated, respectively. We want to say that all the solutions investigated are homogeneous and clear which make us to think that they are in the L2 region of the phase diagram.

It is worthy to mention here that it was not possible to encapsulate EL in the AOT/*n*-heptane systems without the presence of water since the DLS data show no correlation and the polidispersity index was equal to 1. Also, as EL is completely soluble in *n*-heptane it was possible to dissolve EL as the major component in the mixture being *n*-heptane and AOT the minor components and, the DLS data show no correlation as in the other case. Thus, there is not an organized system such as RMs for the EL/AOT/*n*-heptane or for *n*-heptane/AOT/EL mixtures and the systems are only non-structured microemulsions (nonorganized systems).[5]

Parts A and B of Figure 1 report the apparent droplets sizes values obtained in the EL–water/AOT/*n*-heptane media

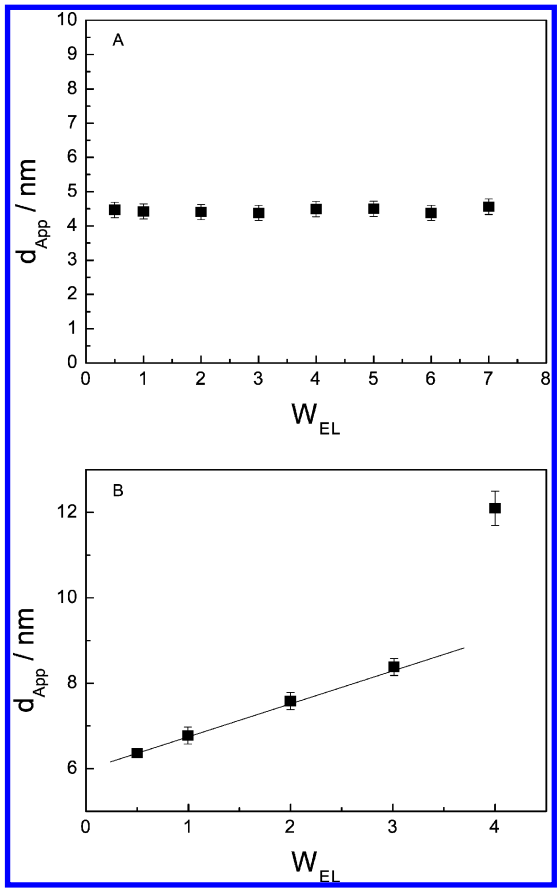

Figure 1. Droplet apparent diameter (d_{App}) variations as a function of W_{EL} for EL–water/AOT/*n*-heptane RMs: (A) W_0 = 5; (B) W_0 = 10. [AOT] = 0.1 M. T = 25 °C.

varying W_{EL} at two different water content (W_0). Figure 1 A corresponds to W_0 = 5 and Figure 1 B corresponds to W_0 = 10. We want to highlight that below W_0 = 5 the DLS data show no presence of AOT RMs since no correlation were obtained. From Figure 1, two different situations can be observed depending on the water content. At low water content (Figure 1A), the droplet size values are independent of the EL amount at every W_{EL} values investigated (even at the maximum W_{EL} value that can be reached to form stable and transparent solution, W_{EL} = 7). The sizes of the droplet (d_{App} = 4.5 nm) correspond to the one obtained for water/AOT/*n*-heptane

dx.doi.org/10.1021/jp311882t | J. Phys. Chem. B 2013, 117, 3818–3828

RMs at W_0 = 5.[1] On the other hand, at higher water content (Figure 1B), the maximum W_{EL} value that can be reached is lower (W_{EL} = 4) than the other case and, the apparent droplet size values increases in a linear tendency with W_{EL} until a value around 3. After that, the size strongly deviates from the linearity probably reflecting the fact that the RMs droplet−droplet interaction is favored changing the shape of the RMs previously to the phase separation value.[35] However, at this point we do not have enough evidence to confirm this assumption.

DLS can be used to assess if the different EL−water mixtures are encapsulated by AOT to create RMs.[5,36−41] Therefore, if the mixture is really encapsulated to form RMs, the droplets size must increase as the W value increases as it is well-established for water or polar solvents/surfactant RMs systems.[1,5,37,38] This feature can also demonstrate that the EL−water/AOT RMs consist (or not) of discrete spherical and noninteracting droplets of the mixture stabilized by the surfactant. If the tendency with W is linear (swelling law of RMs) then the droplet are spherical and noninteracting.[10,39] On the other hand, if the EL−water mixture is not encapsulated by the surfactant the droplets sizes could decrease with the polar solvent addition.[39] In this case, the polar mixture can act as a cosurfactant located in the nonpolar region of the interface, leading to a reduction in the droplets sizes because of the AOT solubility in the nonpolar pseudophase increases, and the cmc value also increases eventually, leading to the RMs' destruction.

It is known that the RMs droplet sizes depend, among many other variables, on the effective packing parameter of the surfactants, v/al_c, in which v and l_c are the volume and the length of the hydrocarbon chain, respectively and a is the surfactant headgroup area. The RMs sizes are larger when the surfactant packing parameter values are smaller.[10] In this sense, we have previously demonstrated[36] that polar solvents that strongly interact with the AOT interface lead to an increase in the effective surfactant headgroup area a. Moreover, it was also demonstrated that the AOT RMs droplet sizes depend strongly on the kind of interactions that the different polar solvents can make with the surfactant rather than their molar volume even when a solvent mixture is confined at a nanoscale size.[10,36] On the other hand, if the interaction between the polar solvent and the interface is small, the droplet size values seem to depend slightly on the polar solvent content.[36]

Our DLS results show two situations depending if the encapsulated water structure corresponds to the bound water (W_0 < 6−8) or to the free water (W_0 > 6−8).[1−3] In the former case when the d_{App} values do not change (Figure 1 A) and correspond to the value obtained for water/AOT/n-heptane RMs, the first explanation that comes out is that EL molecules do not encapsulate and are dissolved in the n-heptane pseudophase (where EL is very soluble). Other possibility never explored before, is that EL molecules are encapsulated by the surfactant but do not interact with the AOT RMs interface because the EL−EL interaction is stronger than water−AOT and EL−AOT interactions. In other word, the polar solvent creates a true polar pool without interacting with the surfactant. Both hypotheses give d_{App} values that do not change with the EL content.

On the contrary, in the second situation when d_{App} increases in a linear tendency with W_{EL} (Figure 1 B), it is clear that EL molecules are encapsulated and interact with the AOT interface probably because once AOT head groups are hydrated the of EL−AOT interactions are greater than EL−EL and water−AOT interactions.

To decide between these possibilities is not an easy task and, a combination of different techniques should be used. In the next sections, we will address a possible answer to the experimental evidence found at different water content.

2.2. 4-AP in EL−Water/AOT/n-Heptane RMs. 2.2.1. Steady-State Absorption and Emission Spectroscopy. In the next sections, we will give an answer to the question of where EL molecules exist within the AOT RMs system using the spectroscopic properties of 4-AP.

4-AP is a molecular probe that is completely insoluble in n-heptane but it can be dissolved in AOT/n-heptane solutions at [AOT] > 0.09 M. Thus, the probe does not undergo a partition process between two different pseudophases in the experimental conditions used in this work.[1,18] Rather than that, 4-AP exists mainly at the AOT RM pseudophase and will monitor the changes of the micelle properties.[42]

Typical 4-AP absorption and emission spectra in EL−water/AOT/n-heptane RMs varying the EL content at W_0 = 10 and [AOT] = 0.1 M are shown in Figure S5, parts A and B, respectively, in the Supporting Information section. Similar features are observed in all the RMs investigated at W_0 above 5 (not shown). Figures 2 A and B summarize the data depicted in Figure S5, Supporting Information, and show the variation of the B1 maxima absorption band, λ_{maxB1} (Figure 2 A) and, the emission maxima, λ_{maxem}, values (λ_{exc} = B1 maximum band,

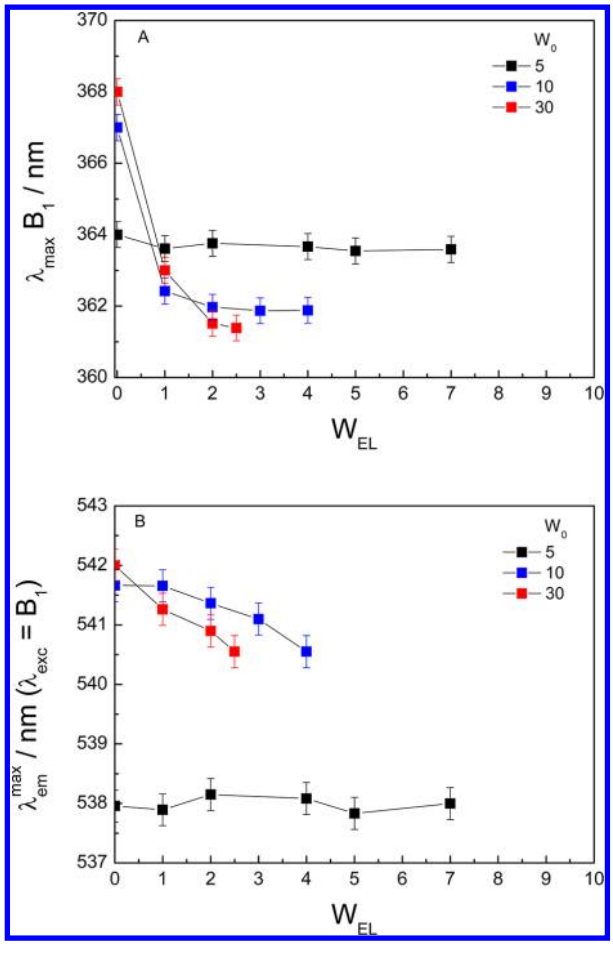

Figure 2. (A) Maxima wavelength values of B_1 absorption band as a function of W_{EL} and (B) maxima wavelength values (λ_{exc} = B1 maximum band) of the emission band as a function of the W_{EL}, at different W_0 values. [AOT] = 0.1 M. [4-AP] = 1 × 10^{-4} M.

dx.doi.org/10.1021/jp311882t | J. Phys. Chem. B 2013, 117, 3818−3828

Figure 2B) for 4-AP in EL−water/AOT/*n*-heptane RMs varying W_{EL} at different water content. First we will discuss the data at different W_0 values with no EL addition, W_{EL} = 0, that are shown in the *y* axis of Figures 2, parts A and B. It can be seen that 4-AP detects water molecules at the AOT RMs interface because of the red shift in the absorption and emission bands observed upon the W_0 values increase.[18,19] The B1 absorbance maxima is λ^{max}_{abs} = 362 nm at W_0 = 0 (no water addition) and shifts to λ^{max}_{abs} = 368 nm at W_0 = 30 while, the emission maxima exciting at the B1 absorption maxima go from λ^{max}_{em} = 447 nm at W_0 = 0 to λ^{max}_{em} = 542 nm at W_0 = 30. It must be noted that the absorbance and emission maxima obtained at W_0 = 30 are close to the values for 4-AP in pure water: λ^{max}_{abs} B1= 370 nm and λ^{max}_{em} = 545.7 nm[23,27] which reflects the sensibility of the molecular probe to the water structure upon encapsulation. Similar shifts were found in the literature but working at excitation wavelength that correspond to the B2 absorption band.[18]

On the other hand, the situation is different when EL is added to the system. From Figure 2, it can be seen that the spectroscopic data give results according to the ones obtained through DLS. At W_0 = 5 where the droplet sizes do not change with W_{EL} values (Figure 1A), 4-AP does not detect EL molecules neither in the absorbance nor in the emission spectra. Parts A and B of Figure 2 show that the band positions are the same with and without EL addition, which means that 4-AP only detects water molecules at the AOT RMs interface. On the other hand, at higher water content, i.e., W_0 = 10 and 30 where the droplet sizes increases with the EL amount (Figure 1 B), it can be observed a noticeable blue shift of the absorption and emission maxima values with W_{EL}. Consequently, 4-AP now senses the presences of EL molecule, which is a solvent with lower polarity in comparison with water (see part 1 of this section), at the AOT RMs interface.

2.2.2. Excitation Wavelength Study on 4-AP. The fact that water is the only solvent where 4-AP emission maxima wavelengths are different depending on the excitation wavelength used in the red-edge of the B1 absorption band (emission blue shift of around 35 nm),[27] motivates us to perform a detailed investigation of this effect in the EL−water/AOT/*n*-heptane RMs to gain more insights about the interface composition. It is known that in bulk nonviscous solvents, dipolar solvent relaxation around the fluorophore in the excited state occurs on a time scale much faster than the fluorophore fluorescence lifetime. However, if the dipolar relaxation of the solvent molecules in the excited state is slow enough that the relaxation time is comparable to or longer than the fluorescence lifetime, then λ^{max}_{emi} will shift toward lower energy (red shift) as the excitation wavelength energy decreases. This effect, known as red edge excitation shift (REES),[15,43] directly monitors the microenvironment and dynamics around a fluorophore in motionally restricted media such as RMs.[44−46] It is important to highlight that the REES effect shifts the emission band to lower energy (red shift) and it is not the explanation for the blue shift found in water of the 4-AP emission maxima when the excitation wavelength is changed in the red-edge of the B1 absorption band. Rather than this effect, the explanation was based in the two 4-AP emitting species found in water (Scheme 2).[27]

In the AOT RMs the situation is different. First we will present the results in the RMs at W_{EL} = 0 and varying the water content. Figure S6A, in the Supporting Information, shows the 4-AP emission spectra in AOT/*n*-heptane RMs at different excitation wavelengths at the red-edge of the B1 absorption band at W_0 = 0. Figure S6B, in the Supporting Information, shows the difference in the emission maximum wavelength when exciting at 420 and 360 nm, $\Delta\lambda^{max}_{em} = \lambda^{max}_{em}$ (λ_{exc} = 420 nm) − λ^{max}_{em} (λ_{exc} = 360 nm), for 4-AP in water/AOT/*n*-heptane at different W_0 values. It can be seen that the emission band shifts to the red in the RMs at W_0 = 0 since the $\Delta\lambda^{max}_{em}$ value is positive. Moreover, a $\Delta\lambda^{max}_{em} \sim$ 24 nm found reflects the motionally constrained environment that 4-AP senses in the AOT RMs interface. Upon water addition it can be seen (Figure S6B, Supporting Information) that at W_0 values <5, $\Delta\lambda^{max}_{em}$ decreases suggesting that the dye's environment becomes significantly more fluid because of the interface hydration.[45] It is interesting what happens at W_0 > 5 where $\Delta\lambda^{max}_{em}$ has negative values of around −14 nm independently on the W_0 investigated. A negative value for $\Delta\lambda^{max}_{em}$ means that the emission band shifts to higher energy (blue shift) as the excitation wavelength is changed to lower energy, result that cannot be attributed to *REES* effect as it was explained and, such blue shift was observed for 4-AP only in water environment[27] with the explanation given in the section of solvent mixtures. Please note that $\Delta\lambda^{max}_{em}$ value found in the AOT RMs is not the same than the one obtained in pure water (∼35 nm) because in the RMs media the *REES* effect is also present with an opposite tendency of the shifts. In this way the dye is suitable to monitor changes at the AOT RMs interface because the fluidity and the water content can be followed at the same time.

The 4-AP behavior in AOT RMs changes in the presence of EL. Parts A and B of Figure 3 show the difference in the emission maximum wavelength when exciting at 420 and 360 nm, $\Delta\lambda^{max}_{em} = \lambda^{max}_{em}$ (λ_{exc} = 420 nm) − λ^{max}_{em} (λ_{exc} = 360 nm) as a function of W_{EL}, for 4-AP in EL−water/AOT/*n*-heptane media at W_0 = 5 and W_0 = 10, respectively. As expected at W_0 = 5, 4-AP only detects the presence of water at the AOT RMs interface independently on W_{EL} values. This come out since $\Delta\lambda^{max}_{em}$ values are the same than the one obtained at W_{EL} = 0 (Figure S6B, Supporting Information). On the other hand, at W_0 = 10 $\Delta\lambda^{max}_{em}$ values drops markedly to a value of −6.9 as the EL content increases. With this amount of water 4-AP senses the presence of EL molecules at the AOT RMs interface.

Interestingly, the data shown in Figure 3 demonstrate that the interfacial water present in the AOT RMs can also help to the solvent mediated proton transfer reaction that the keto 4-AP −ICT species undergoes in pure water (Scheme 2). On the other hand, for W_0 values higher than 5, the presence of EL at the interface seems to difficult the proton transfer process because the $\Delta\lambda^{max}_{em}$ significantly reduces the value.

To confirm where the EL molecules are located within the RMs, we study the 4-AP behavior using time-resolved emission measurements under different experimental conditions.

2.2.3. Time-Resolved Emission Spectra (TRES) of 4-AP in EL−water/AOT/n-Heptane RMs. Figure S7A, in the Supporting Information, shows the TRES spectra for 4-AP (at λ_{exc} = B1 maximum band) in AOT/*n*-heptane RMs at $W_0 = W_{EL}$ = 0, that is RMs without water and EL addition. Figure S7B, Supporting Information, shows also TRES spectra for 4-AP in EL−AOT-*n*-heptane systems at EL:AOT molar ratio of 40 and without water addition. The data of EL−AOT-*n*-heptane system is presented, even though the DLS experiments clearly show that for W_0 below 5 RMs are not formed, because we want to explore what the dye senses in a mixture that it is not an organized media.

dx.doi.org/10.1021/jp311882t | J. Phys. Chem. B 2013, 117, 3818−3828

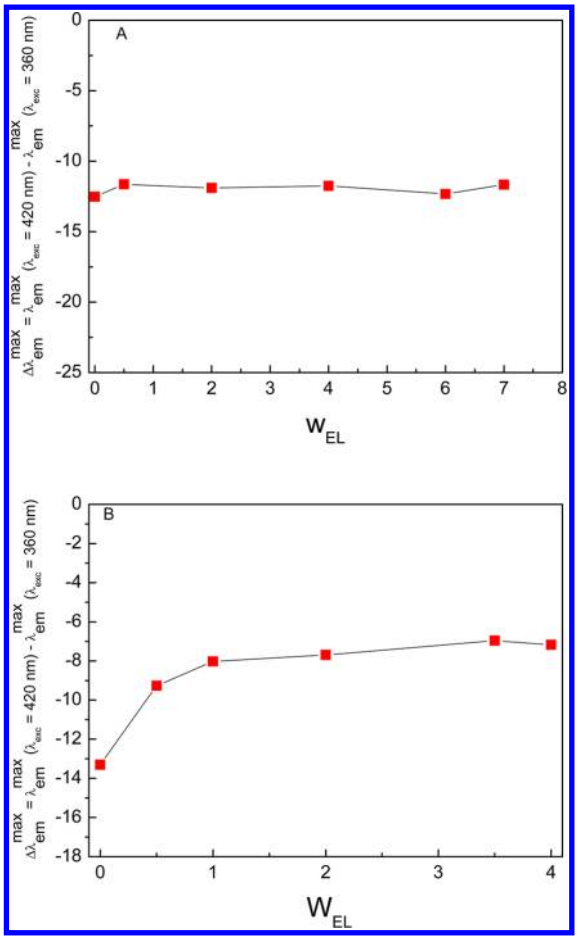

Figure 3. $\Delta\lambda^{max}_{em} = \lambda^{max}_{em}$ (λ_{exc} = 420 nm) − λ^{max}_{em} (λ_{exc} = 360 nm) values for 4-AP in EL−water/AOT/*n*-heptane RMs as a function of W_{EL}. (A) W_0 = 5. (B) W_0 = 10. [AOT] = 0.1 M. [4-AP] = 1 × 10^{-4} M.

Figure S7A, Supporting Information, shows that the emission spectra shift progressively to longer wavelengths increasing time (from λ^{max}_{em} = 447 nm at t = 0.5 ns to λ^{max}_{em} = 465 nm at t = 60 ns) while the band shape shows little or no variation. These facts are in agreement with the continuous model for the spectral relaxation, which can explain TRES that comes from solvent relaxation where the initially excited state (4-AP keto-ICT state (Scheme 2)) relaxes to a solvent relaxed state.[15,16,18] Thus, due to the constrained environment that the AOT RMs interface offers to 4-AP, the solvation dynamics slows down and it can be detected in our nanosecond setup at W_0 = 0. On the other hand, Figure S7B, Supporting Information, shows that there is no dependence of the TRES spectra with time in the EL−AOT-*n*-heptane system, which indicates that the solvation dynamics is too fast to be detected in our equipment and, that 4-AP emits from the relaxed keto-ICT state (Scheme 2). Moreover, the emission maxima wavelength (λ^{max}_{em} = 519 nm) and the spectra shape match the results obtained in the 1:1 EL−*n*-heptane mixture (Figure S4B,Supporting Information). This indicates that 4-AP is preferentially solvated by EL even in the complex mixture of AOT, *n*-heptane and EL molecules and, confirms the results obtained through DLS that this mixture is not an organized system. The same trend was observed at other EL:AOT molar ratio investigated: 4, 10, and 20 (results not shown) and even with water dissolved in the mixture up to a molar ratio to the surfactant concentration of 5 (not shown).

The next step before going to more complex RMs, is to show the results in the water/AOT/*n*-heptane RMs without EL addition (W_{EL} = 0) at different water content. Figure S8A, Supporting Information, shows typical TRES spectra of 4-AP in water/AOT/*n*-heptane RMs at W_0 = 30 and Figure S8B, Supporting Information, which is obtained from the TRES spectra at different W_0 values, shows the difference in the emission maximum wavelength at times 60 and 0.5 ns, $\Delta\lambda^{max}_{em} = \lambda^{max}_{em}$ (t = 60 ns) − λ^{max}_{em} (t = 0.5 ns), as a function of W_0. As it can be observed and similarly to what it was found in pure water,[27] in the AOT RMs when water is present the emission spectra shift markedly to shorter wavelengths and the band shape narrows on increasing the time (Figure S8A, Supporting Information). Clearly, the presence of water in the RMs interface helps in the solvent mediated proton transfer reaction that 4-AP keto-ICT species undergoes yielding the 4-AP enol-ICT species. Both species are then responsible of the 4-AP emission profile (Scheme 2) as it was discussed in pure water.[27] The narrowing of the band is more notorious in the AOT RMs system than in water,[27] which suggests that the 4-AP enol-ICT conversion is favored at the AOT RMs interface. It is worthy to note that the enol-ICT species has a good hydrogen donor group (the enol OH) and as it is well-known, the AOT interface is very good accepting hydrogen bond interactions.[1,47]

Finally we present the results obtained for the more complex RMs: EL−water/AOT/*n*-heptane RMs. Parts A and B of Figure S9 in the Supporting Information show typical TRES spectra of 4-AP in EL−water/AOT/*n*-heptane RMs at W_0 = 5, W_{EL} = 6 and W_0 = 10, and W_{EL} = 4, respectively. Parts A and B of Figure 4 show the difference in the emission maximum wavelength at times 60 and 0.5 ns, $\Delta\lambda^{max}_{em} = \lambda^{max}_{em}$ (t = 60 ns) - λ^{max}_{em} (t = 0.5 ns), as a function of W_{EL} at W_0 = 5 and 10, respectively. In the figures, it is clear that the blue shift that 4-AP emission band undergoes with time is smaller at W_0 = 10 because the probe detects EL molecules at the interface. At W_0 = 5, the dye only feels water molecules at any EL content, as was discussed.

From Figure 4A, we can infer that at W_0 = 5 EL molecules exists inside the AOT RMs and they are not dissolved in the *n*-heptane pseudophase, because of 4-AP emission band shifts to the blue. We have shown in Figure S6B, Supporting Information, that when EL is dissolved in a nonstructured microemulsion media, the 4-AP blue shift is not detected. Thus, the possibility that EL molecules go to the *n*-heptane pseudophase is discarded.

Scheme 3 summarizes the above discussion. We have shown in concordance with the literature,[13] that EL is a liquid that show strong intermolecular association and competes for intramolecular hydrogen bonding. In water mixtures, addition of small quantities of EL to liquid water has a strong effect on the water structure reinforcing the water networks and diminishing the water−EL interaction. This situation in AOT RMs occurs when W_0 is higher than 10 and the system has free water molecules in the pool.[1] Hence, it is likely that at W_0 = 10 the water − AOT interaction diminishes because there is enough water to break the EL−EL interaction and there is EL at the RMs interface. That is, EL molecules go to the interface to interact with AOT polar headgroup. Thus, the surfactant packing parameter is changed and the RMs droplet sizes are bigger.

On the other hand, as it was discussed in the part 1 of this section, the results for the EL-rich region show that the water addition has practically no effect on the EL structure. In AOT RMs media this is equivalent to the data discussed at low water

dx.doi.org/10.1021/jp311882t | J. Phys. Chem. B 2013, 117, 3818−3828

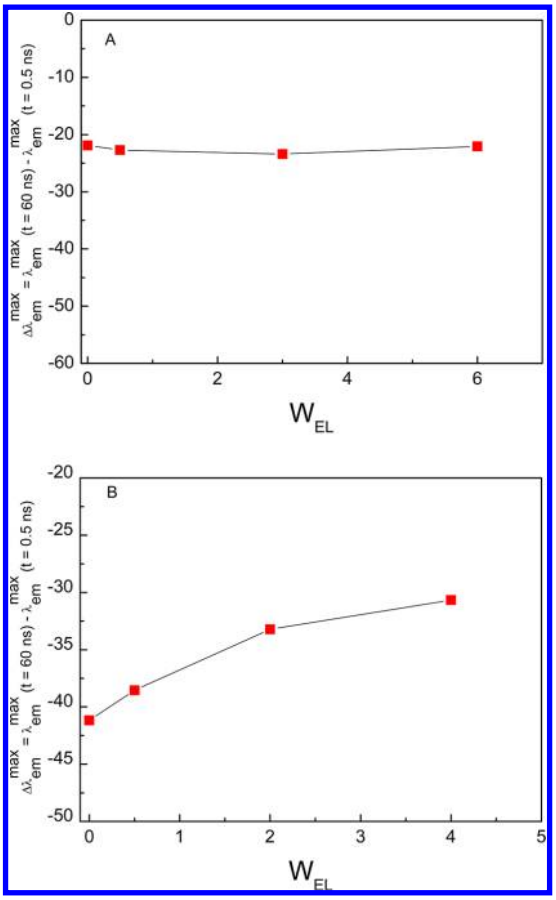

Figure 4. $\Delta\lambda^{max}_{em} = \lambda^{max}_{em}$ (t = 60 ns) − λ^{max}_{em} (t = 0.5 ns) values for 4-AP in EL−water/AOT/*n*-heptane RMs as a function of W_{EL} at (A) W_0 = 5 and (B) W_0 = 10. λ_{exc} = 378 nm (B_1 maximum band). [AOT] = 0.1 M. [4-AP] = 1 × 10^{-4} M.

content, W_0 = 5. Herein, EL−EL interaction is stronger than EL−water interaction and, the interfacial bound water strongly interacts with AOT polar head and gives an interface with no EL molecules. Because of the strong EL−EL interaction they can form an EL pool in the AOT RMs.

However, for W_0 values smaller than 5, the very little amount of water and the presence of larger amount of EL molecules prevents the formation of the AOT RMs. Instead of this the mixture forms a nonstructured mixture (nonorganized systems) as it is shown in Scheme 3. Under this scenario any amount of EL can be dissolved which makes impossible to determine a maximum value for W_{EL}.

CONCLUSIONS

The unique behavior of 4-AP under the presence of water molecules motivate us to perform a detail investigation of the EL−water mixture and the effect that the constrained environment has on this interaction. Thus, we investigate the EL−water/AOT/*n*-heptane system using DLS, absorbance and steady-state and time-resolved emission spectroscopy. We show that 4-AP is very useful not only to detect preferential solvation in homogeneous media but, to monitor the presence or the absence of organized media such as AOT RMs. Also, it helps to clearly detect where the polar solvents exist within the RMs.

Our results demonstrate that in homogeneous media, water molecules preferential solvates the solvent shell sphere of 4-AP, while in EL−*n*-heptane mixtures 4-AP is always solvate by EL molecules through hydrogen bond interaction. With the presence of AOT the situation is different. DLS and spectroscopic experiments show that below W_0 = 5 values, there is no RMs and EL, water, AOT and *n*-heptane forms a nonstructured mixture. For W_0 values between 5 and 10, the droplet sizes values are independent of the EL content because EL molecules interact strongly with each other forming an EL polar pool. For W_0 values larger than 10, the droplets size values increase with the EL content because of EL molecules interact with the AOT RMs interface.

These results, give a strong evidence about which are the factors that determine the RMs droplet sizes depending on the structure of encapsulated polar solvent, giving insights that help to control the sizes of the AOT RMs.

Scheme 3. Cartoon with the Representation of the Estimated Different Location for EL and Water in EL−Water/AOT/*n*-Heptane Systems, at Different Water Content

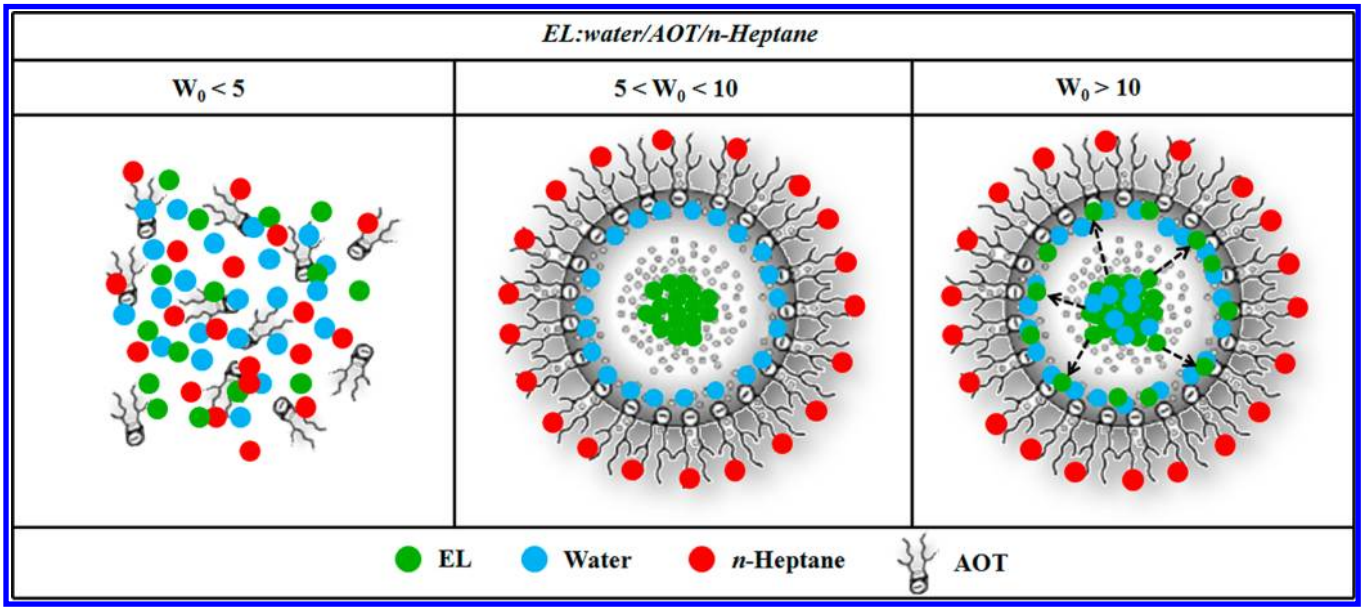

dx.doi.org/10.1021/jp311882t | J. Phys. Chem. B 2013, 117, 3818−3828

■ ASSOCIATED CONTENT

Supporting Information

Figure S1, absorption and emission spectra of 4-AP in pure solvents; Figure S2, frequencies of the absorption maxima of B_1 and B_2 bands as a function of X_{water} and $X_{n\text{-Hp}}$ and frequencies of the emission maxima at λ_{exc} = B1 a function of X_{water} and $X_{n\text{-Hp}}$; Figure S3, dependence of the emission wavelength (λ^{max}_{em}) with the excitation wavelength (λ_{exc}) at the red-edge of the B1 band for different EL:water and EL:*n*-Hp mixtures composition; Figure S4, normalized TRES of 4-AP in EL−water, EL and in the 1:1 EL−*n*-Heptane mixture; Figure S5, absorption spectra of 4-AP in the system EL−water/AOT/*n*-heptane and, emission spectra of 4-AP in the system EL−water/AOT/*n*-heptane, as a function of W_{EL}; Figure S6, emission spectra of 4-AP in AOT/*n*-heptane RMs at W_0 = W_{EL} = 0 at different excitation wavelengths at the red-edge of the B_1 band, with different $\Delta\lambda^{max}_{em} = \lambda^{max}_{em}$ (λ_{exc} = 420 nm) − λ^{max}_{em} (λ_{exc} = 360 nm) values at different λ_{exc} for 4-AP in water/AOT/*n*-heptane RMs as a function of W_0 with W_{EL} = 0; Figure S7, normalized TRES spectra of 4-AP in AOT/*n*-heptane at W_0 = W_{EL} =0 and in EL/AOT/*n*-heptane at W_{EL} = 40, W_0 = 0; Figure S8, normalized TRES spectra of 4-AP in water/AOT/*n*-heptane at W_0 = 30; $\Delta\lambda^{max}_{em} = \lambda^{max}_{em}$ (t = 60 ns) − λ^{max}_{em} (t = 0.5 ns) values as a function of W_0; Figure S9, normalized TRES spectra of 4-AP in EL−water/AOT/*n*-heptane at W_0 = 5, W_{EL} = 6 and W_0 = 10, W_{EL} = 4. This material is available free of charge via the Internet at http://pubs.acs.org.

■ AUTHOR INFORMATION

Corresponding Author

*(N.M.C.) E-mail: mcorrea@exa.unrc.edu.ar. Telephone/fax: 54-358-4676233.

Notes

The authors declare no competing financial interest.

■ ACKNOWLEDGMENTS

We gratefully acknowledge the financial support for this work by the Consejo Nacional de Investigaciones Científicas (CONICET), Agencia Córdoba Ciencia, Agencia Nacional de Promoción Científica y Técnica and Secretaría de Ciencia y Técnica de la Universidad Nacional de Río Cuarto. N.M.C., J.J.S. and R.D.F. hold a research position at CONICET. A.M.D. thanks CONICET for a research fellowship.

■ REFERENCES

(1) Silber, J. J.; Biasutti, M. A.; Abuin, E.; Lissi, E. Interaction of Small Molecules with Reverse Micelles. *Adv. Colloid Interface Sci.* **1999**, *82*, 189−252.

(2) De, T. K.; Maitra, A. Solution Behavior of Aerosol-OT in Nonpolar-Solvents. *Adv. Colloid Interface Sci.* **1995**, *59*, 95−193.

(3) Moulik, S. P.; Paul, B. K. Structure, Dynamics and Transport Properties of Microemulsions. *Adv. Colloid Interface Sci.* **1998**, *78*, 99−195.

(4) Hazra, P.; Chakrabarty, D.; Sarkar, N. Intramolecular Charge Transfer and solvation Dynamics of Coumarin 152 in Aerosol-OT, Water-Solubilizing Reverse Micelles, and Polar Organic Solvent Solubilizing Reverse Micelles. *Langmuir* **2002**, *18*, 7872−7879.

(5) Correa, N. M.; Silber, J. J.; Riter, R. E.; Levinger, N. E. Nonaqueous Polar Solvents in Reverse Micelle Systems. *Chem. Rev.* **2012**, *112*, 4569−4602.

(6) Sengwa, R. J.; Khatri, V.; Sankhla, S. Dielectric Properties and Hydrogen Bonding Interaction Behaviour in Binary Mixtures of Glycerol with Amides and Amines. *Fluid Phase Equilib.* **2008**, *266*, 54−58.

(7) Zielkiewicz, J. Preferential Solvation of N-methylformamide, N,N-Dimethylformamide and N-Methylacetamide by Water and Alcohols in the Binary and Ternary Mixtures. *Phys. Chem. Chem. Phys.* **2000**, *2*, 2925−2932.

(8) Santo, M.; Anunziata, J. D.; Cattana, R.; Silber, J .J. Solvatochromic Studies in Quinoline and Cyanoquinoline. Preferential Solvation in Alcohol-Cyclohexane Benary Mixtures. *Spectrochim. Acta, A.* **1995**, *51*, 1749−1749.

(9) Reichardt, C. *Solvents and Solvent Effects in Organic Chemistry*; 3rd ed.; VCH: Weinheim, Germany, 2003.

(10) Durantini, A. M.; Falcone, R. D.; Silber, J. J.; Correa, N. M. A New Organized Media: Glycerol:N,N-Dimethylformamide Mixtures/AOT/n-Heptane Reversed Micelles. The Effect of Confinement on Preferential Solvation. *J. Phys. Chem. B* **2011**, *115*, 5894−5902.

(11) Aparicio, S.; Alcalde, R. Insights into the Ethyl Lactate + Water Mixed Solvent. *J. Phys. Chem. B* **2009**, *113*, 14257−14269.

(12) Warner, J. C.; Cannon, A. S.; Dye, K. M. Green Chemistry. *Environ. Impact Assess. Rev.* **2004**, *24*, 775−799.

(13) Aparicio, S.; Halajian, S.; Alcalde, R.; García, B.; Leal, J. M. Liquid Structure of Ethyl Lactate, Pure and Water Mixed, as seen by Dielectric Spectroscopy, Solvatochromic and Thermophysical Studies. *Chem. Phys. Lett.* **2008**, *454*, 49−55.

(14) Aparicio, S.; Alcalde, R. The Green Solvent Ethyl Lactate: An Experimental and Theoretical Characterization. *Green Chem.* **2009**, *11*, 65−78.

(15) Lakowicz, J. R. *Principles of Fluorescence Spectroscopy*, 3rd ed., Springer: New York, 2006.

(16) Wetzler, D. E.; Chesta, C.; Fernández-Prini, R.; Aramendía, P. F. Dynamic Solvation of Aminonaphthalimides in Solvent Mixtures. *J. Phys. Chem. A* **2002**, *106*, 2390−2400.

(17) Krystokowiak, E.; Dobek, K.; Maciejewski, A. Origin of the Strong Effect of Protic Solvents on the Emission Spctra, Quantum Yield of Fluorescence and Fluorescence Lifetime of 4-Amino-phthalimide. Role of Hydrogen Bonds in Deactivaation of S_1−4-aminophthalimide. *J. Photochem. Photobiol. A: Chem.* **2006**, *184*, 250−264.

(18) Das, S.; Datta, A.; Bhattacharyya, K. Deuterium Isotope Effect on 4-Aminophthalimide in Neat Water and Reverse Micelles. *J. Phys. Chem. A* **1997**, *101*, 3299−3304.

(19) Harju, T. O.; Hizer, A. H.; Varma, C. Non-Exponential Solvation Dynamics of Electronically Excited 4-Aminophthalimide in *n*- Alcohols. *Chem. Phys.* **1995**, *200*, 215−224.

(20) Kim, T. G.; Wolford, M. F.; Topp, M. R. Ultrashort-Lived Excited States of Aminophthalimides in Fluid Solution. *Photochem. Photobiol. Sci.* **2003**, *2*, 572−584.

(21) Paul, A.; Samanta, A. Solute Rotation and Solvation Dynamics in an Alcohol-Functionalized Room Temperature Ionic Liquid. *J. Phys. Chem. B* **2007**, *111*, 4724−4731.

(22) Barja, B. J.; Chesta, C.; Atvards, T. D. Z.; Aramendia, P. F. Relaxations in Poly(vinyl alcohol) and in Poly(vinyl acetate) Detected by Fluorescence Emission of 4-Aminophthalimide and Prodan. *J. Phys. Chem. B* **2005**, *109*, 16180−16187.

(23) Murkherjee, S.; Sahu, K.; Roy, D.; Mondal, S. K.; Bhattacharyya, K. Solvation Dynamics of 4-Aminophthalimide in Dioxane-Water Mixture. *Chem. Phys. Lett.* **2004**, *384*, 128−133.

(24) Bhattacharyya, K. Nature of Biological Water: A Femtosecond Study. *Chem. Commun.* **2008**, *25*, 2848−2857.

(25) Maciejewski, A.; Kubicki, J.; Dobek, K. Different Sources of 4-Aminophthalimide Solvation Dynamics Retardation Inside Micellar Systems. *J. Colloid Interface Sci.* **2006**, *295*, 255−263.

(26) Wang, R.; Hao, C.; Li, P.; Wei, N.-G.; Chen, J.; Qiu, J. Time-Dependent Density Functional Theory Study on the Electronic Excited-State Hydrogen-Bonding Dynamics of 4-Aminophthalimide (4AP) in Aqueous Solution: 4AP and 4AP−$(H_2O)_{1,2}$ Clusters. *J. Comput. Chem.* **2010**, *31*, 2157−2163.

(27) Durantini, A. M.; Falcone, R. D.; Anunziata, J. D.; Silber, J. J.; Abuin, E. B.; Lissi, E. A.; Correa, N. M. An Interesting Case where Water Behaves as a Unique Solvent. 4-Aminophthalimide Emission

Profile to Monitor Aqueous Environment. *J. Phys. Chem. B* **2013**, *117*, 2160−2168.
(28) Correa, N. M.; Biasutti, M. A.; Silber, J. J. Micropolarity of Reverse Micelles of Aerosol-OT in *n*-Hexane. *J. Colloid Interface Sci.* **1995**, *172*, 71−76.
(29) Correa, N. M.; Biasutti, M. A.; Silber, J. J. Micropolarity of Reversed Micelles: Comparison between Anionic, Cationic, and Nonionic Reversed Micelles. *J. Colloid Interface Sci.* **1996**, *184*, 570−578.
(30) O'Connor, D. V.; Phillips, D. *Time-Correlated Single Photon Counting*; Academic Press: New York, 1983; Chapter 6.
(31) Maroncelli, M. P.; Fleming, J. R. Picosecond Solvation Dynamics of Coumarin-153 - The Importance of Molecular Aspects of Solvation. *J. Chem. Phys.* **1987**, *86*, 6221−6239.
(32) Suppan, P. Local Polarity of Solvent Mixtures in the Field of Electronically Excited Molecules and Exciplexes. *J. Chem. Soc., Faraday Trans. 1* **1987**, *83*, 495−509.
(33) Kamlet, M. J.; Abboud, J. L. M.; Abraham, M. H.; Taft, R. W. J. Linear solvation energy relationships. 23. A comprehensive collection of the solvatochromic parameters, π^*, α, and β, and some methods for simplifying the generalized solvatochromic equation. *J. Org. Chem.* **1983**, *48*, 2877−2887.
(34) Salabat, A.; Eastoe, J.; Mutch, K. J.; Rico, F. Tabor. Tuning Aggregation of Microemulsion Droplets and Silica Nanoparticles using Solvent Mixtures. *J. Colloid Interface Sci.* **2008**, *318*, 244−251.
(35) Agazzi, F. M.; Falcone, R. D.; Silber, J. J.; Correa, N. M. Solvent Blends can Control Cationic Reversed Micellar Interdroplet Interactions. The Effect of n-Heptane:Benzene Mixture on BHDC Reversed Micellar Interfacial Properties: Droplet Sizes and Micropolarity. *J. Phys. Chem. B* **2011**, *115*, 12076−12084.
(36) Falcone, R. D.; Silber, J. J.; Correa, N. M. What are the Factors that Control non-Aqueous/AOT/*n*-Heptane Reverse Micelle Sizes? A Dynamic Light Scattering Study. *Phys. Chem. Chem. Phys.* **2009**, *11*, 11096−11100.
(37) Fletcher, P. D. I.; Galal, M. F.; Robinson, B. H. Structural Study of AOT Stabilised Microemulsions of Glycerol Dispersed in n-Heptane. *J. Chem. Soc., Faraday Trans. I* **1984**, *80*, 3307−3314.
(38) Riter, R. E.; Undiks, E. P.; Kimmel, J. R.; Levinger, N. E. Formamide in Reverse Micelles: Restricted Environment Effects on Molecular Motion. *J. Phys. Chem B* **1998**, *102*, 7931−7938.
(39) Riter, E. R.; Kimmel, J. R.; Undiks, E. P.; Levinger, N. E. Novel Reverse Micelles Partitioning Nonaqueous Polar Solvents in a Hydrocarbon Continuous Phase. *J. Phys. Chem. B* **1997**, *101*, 8292−8297.
(40) Eastoe, J.; Gold, S.; Rogers, S. E.; Paul, A.; Welton, T.; Heenan, R. K.; Grillo, I. Ionic Liquid-in-Oil Microemulsions. *J. Am. Chem. Soc.* **2005**, *127*, 7302−7303.
(41) Gao, Y.; Li, N.; Zheng, L.; Bai, X.; Yu, L.; Zhao, X.; Zhang, J.; Zhao, M.; Li, Z. Role of Solubilized Water in the Reverse Ionic Liquid Microemulsion of 1-Butyl-3-methylimidazolium Tetrafluoroborate/TX-100/Benzene. *J. Phys. Chem. B* **2007**, *111*, 2506−2513.
(42) Falcone, R. D.; Correa, N. M.; Silber, J. J. On the Formation of New Reverse Micelles: A Comparative Study of Benzene/Surfactants/Ionic Liquids Systems Using UV-Visible Absorption Spectroscopy and Dynamic Light Scattering. *Langmuir* **2009**, *25*, 10426−10429.
(43) Milhaud, J. New Insights into Water-Phospholipid Model Membrane Interactions. *Biochim. Biophys. Acta* **2004**, *1663*, 19−51.
(44) Chattopadhyay, A.; Mukherjee, S. Fluorophore Environments in Membrane-Bound Probes: a Red Edge Excitation Shift Study. *Biochemistry* **1993**, *32*, 3804−3811.
(45) Correa, N. M.; Levinger, N. E. What Can You Learn from a Molecular Probe? New Insights on the Behavior of C343 in Homogeneous Solutions and AOT Reverse Micelles. *J. Phys. Chem. B* **2006**, *110*, 13050−13061.
(46) Chattopadhyay, A. Exploring Membrane Organization and Dynamics by the Wavelength-Selective Fluorescence Approach. *Chem. Phys. Lipids* **2003**, *122*, 3−17.
(47) Silva, O. F.; Fernández, M.; Silber, J. J.; de Rossi, R. H.; Correa, N. M. Inhibited Phenol Ionization in Reverse Micelles. Confinement Effect at the Nanometric Scale. *ChemPhysChem* **2012**, *13*, 124−130.